Original Research Article
ISSN: **3041-5357**
Journal homepage: https://diversity.researchfloor.org/

Journal of Diversity Studies

Green Synthesis of Silver Nanoparticles Using *Wrightia tinctoria* Pod Extract and Evaluation of Their Anti-Adipogenic Activity in 3T3-L1 Cells

Arpana Ashokrao Durge[1,3], Utkarsh Ravindra Moon[2] and Utpal Jagdish Dongre*[3]

[1]*Department of Biochemistry, Guru Nanak College of Science, Ballarpur, District Chandrapur, Maharashtra, – 442701, India*
[2]*Department of Microbiology and Biotechnology, Mahatma Gandhi College of Science, Gadchandur, District Chandrapur, Maharashtra, – 442908, India*
[3]*Department of Biochemistry and Biotechnology, Dr. Ambedkar College, Deekshabhoomi, Nagpur, Maharashtra, – 440010, India (Affiliated to Rashtrasant Tukadoji Maharaj Nagpur University, Nagpur)*

ABSTRACT

This research investigates the green synthesis of silver nanoparticles (AgNPs) using Wrightia tinctoria pod extracts and evaluate their anti-adipogenic activity in 3T3-L1 cells. Formation of AgNPs was initially confirmed by the appearance of dark brown colour and was later confirmed by UV-Visible spectroscopy of the sample. FTIR studyconfirmed localization of functional groups from the plant that participated in the reduction, stabilization and formation of the AgNPs. XRD analysis showed crystalline nature of nanoparticles and the characteristic reflections of face centered cubic silver crystallite size was 93 nm in average. The EDX analysis revealed the major element to be silver, and the SEM analysis indicated aggregation of particles. The TEM results showed spherical to quasi-spherical in shape with 30.4 nm average size. The particle size ranges from 19.97 to 43.89 nm. MTT assay showed that it was concentration-dependent and showed an estimated IC_{50} of 119.7 µg/mL. AgNPs at the concentration lower than IC_{50}caused a reduced intracellular lipid accumulation in differentiated 3T3-L1 adipocytes. The 57.17%, 45.18% and 42.00% relative lipid accumulation at 80, 100 and 120 µg/mL, respectively, was observed using an Oil Red O staining method compared with the untreated control. The results prove that the extract from W. tinctoria pods can act as a plant derived reducing and stabilizing agent for AgNP synthesis, and the obtained AgNPs have initial anti-adipogenic activity which reduces the accumulation of lipids in 3T3-L1 cells.

Keywords: *Wrightia tinctoria, silver nanoparticles, green synthesis, anti-adipogenic activity, 3T3-L1 cells, MTT assay..*

Citation: Arpana Ashokrao Durge, Utkarsh Ravindra Moon and Utpal Jagdish Dongre [2026]. Green Synthesis of Silver Nanoparticles Using *Wrightia tinctoria* Pod Extract and Evaluation of Their Anti-Adipogenic Activity in 3T3-L1 Cells. *Journal of Diversity Studies.*
DOI: https://doi.org/10.51470/JOD.2026.5.2.235

Corresponding Author: *Utpal Jagdish Dongre*

E-mail Address: *utpal24dongre@gmail.com*

Article History: *Received 13 May 2026 | Revised 15 June 2026 | Accepted 16 July 2026 | Available Online August 14, 2026*

Copyright: *© 2026 by the author. The license of Journal of Diversity Studies. This article is an open access article distributed under the terms and conditions of the Creative Commons Attribution (CC BY) license* ***(https://creativecommons.org/licenses/by/4.0/).***

Introduction

Obesity is a metabolic disorder which is caused by the deposition of excess fat tissue in the body and is related to various complexities such as diabetes mellitus type 2, cardiovascular diseases and hypertension [1]. The expansion of adipose tissue is achieved by adipocyte hypertrophy, hyperplasia, and adipogenesis, the process of converting preadipocytes to mature adipocytes, is essential for the accumulation of lipids and occurrence of obesity[2].Peroxisome proliferator-activated receptor gamma (PPARγ), and CCAAT/enhancer-binding protein alpha (C/EBPα) transcription factors are activated in adipogenesis, a process that involves adipocyte differentiation and lipid storage [3]. The 3T3-L1 preadipocyte cell line are widely used as cell model for adipogenesis which serves as an ideal platform for screening of antiadipogenic substances [4,5]. Silver nanoparticles (AgNPs), owing to their unique physico-chemical and biological activities, have gained the interest of many researchers. They are small in size, with a large surface to volume ratio that, allows their efficient interaction with biological systems. This ability makes them very useful in biomedical research [6]. Besides their well-documented antimicrobial activity[7,8,9,10], AgNPs may also alter the processes involved in lipid metabolism and adipocyte differentiation [11]. The green synthesis using extracts of bioactive/medicinal plants is an alternative in the nanoparticle biosynthesis, which is also an eco-friendly process [12]. Plant secondary metabolites like phenolics, flavonoids and other reducing compounds can help reduce Ag^+ to Ag^0, and they can also serve as capping and stabilizing agents [13,14,15]. This is a simple, economic and eco-friendly method of nanoparticle production. AgNPs produced from plants can have biological properties because of silver and phytochemicals that are attached to the surface of AgNPs[16]. These biomolecules have the potential to affect the stability of the nanoparticles, surface properties and cell interactions. Hence, the choice of appropriate medicinal plant can be critical for developing biologically active AgNPs.

Wrightia tinctoria or Dye's oleander is a medicinal flowering plant known to possess various phytochemicals such as alkaloids, flavonoids, terpenoids and glycosides[17]. These constituents have shown antioxidant, anti-inflammatory and antimicrobial properties, and could also provide important biological properties to plant-derived nanoparticles. The application of *W. tinctoria* pod extract for synthesis of AgNP is of special relevance as the phytochemicals of *W. tinctoria* can be involved in the biosynthesis of AgNP. These can act as electron donors to silver ions and then stay attached to the surface of the nanoparticle as capping molecules in plant mediated synthesis. Intracellular accumulation of neutral lipids in differentiated adipocytes has been widely evaluated by Oil Red O staining[18]. Anti-adipogenic or anti-lipogenic activity can be suggested by the decrease in the formation of lipid droplets as a result of treatment. Most importantly, cytotoxicity needs to be analysed to differentiate true anti-adipogenic activities from non-specific effects resulting from decreased cell viability [19]. MTT assay is a preliminary evaluation method to study the metabolic state of the cells which identifies safe concentrations of the drug for further biological evaluation[20,21,22]. Different concentrations of AgNPs were then evaluated to study the cytotoxicity before examining their effect on lipid accumulation. Biogenic AgNPs are gaining more and more popularity for their biological activity, but *W. tinctoria*-mediated AgNPs' anti-adipogenic activity has been insufficiently studied. Additional studies are needed to determine if a specific adipogenic pathway is affected by these nanoparticles and if they affect adipocyte differentiation and lipid storage. Thus, this work aims at synthesizing AgNPs using the extract of the *W. tinctoria* pods, characterize the synthesized nanoparticles, assess the cytotoxicity of the synthesized AgNPs in 3T3-L1 cells and evaluate the anti-adipogenic activity by evaluating lipid accumulation within the cells by Oil Red O staining.

Materials and Methods

Plant extract preparation and biogenesis of AgNPs

The protocol was performed according to [7] with some modifications. Fresh pods of *W. tinctoria* were picked, washed with tap water followed by distilled water to wash away dust and impurities that stick to the pods. Shade drying of the cleaned pods was done for about 7 days at 30-35°C. The pods were then completely dried, divided into small pieces and appropriately weighed according to requirements. To prepare methanolic extract, 100 g of crushed and dried *W. tinctoria* pods were placed in 100 mL beaker containing methanol and distilled water (80:20). A stepwise temperature variation was employed for obtaining the extracts. At first, the mixture was kept at 50°C for 1 h and then heated at 100°C for 30 min. The temperature was then raised to 130°C and the heating was carried out until the volume of the extract was about half of the original. An extract was obtained and analysed by extracting it into a dark colour. The pods were extracted in the presence of methanol as explained above and the methanolic extract was incubated overnight. The extract was then centrifuged at 10000 × g for 10 min to remove suspended particles and filtered through a filter paper to remove coarse debris. About 25 mL of clear brown coloured filtrate was obtained for AgNPs synthesis. About, 1.698 g of silver nitrate crystals were dissolved in 100 mL of distilled water to make a 100 mM $AgNO_3$ solution. The filtered *W. tinctoria* pod extract (25 mL) and freshly prepared $AgNO_3$ solution (100 mL) were mixed and stirred for a few minutes. The colour change was noticed (brown), which indicated the AgNPs formation. After the incubation, turbidity increase and formation of dark precipitate was noted at the bottom of the flask followed by centrifugation for 5 min at 10000 × g. Synthesized nanoparticles were collected as a pellet after discarding supernatant. The nanoparticle pellet was cleaned with acetone to get rid of any contaminants and then sprinkled up in the round bottom centrifuge tubes. The purified pellet was poured in a watch glass and left to dry overnight.

Characterization of green synthesised AgNPs

Silver nanoparticles (AgNPs) biosynthesized using extract from pods of *Wrightia tinctoria* were characterized by UV–Visible spectroscopy, Fourier-transform infrared spectroscopy (FTIR), X-ray diffraction (XRD), scanning electron microscopy coupled with energy-dispersive X-ray analysis (SEM–EDX) and high-resolution transmission electron microscopy (HRTEM). The monitoring AgNPs synthesis was done by measuring the optical density (400-800 nm) of the solution in the UV–Visible spectrophotometer (UV-1780, Shimadzu, Japan). FTIR spectroscopy was done using Thermo Scientific Nicolet iS50 FTIR spectrometer with ATR–diamond crystal accessory in the spectral range of 4000–400 cm^{-1}. The crystalline structure of AgNPs is studied by a powder X-ray diffractometer, Bruker D8 Advance, Germany using Cu Kα radiation (λ = 1.5406 Å) with 2θ range of 10–80°. The surface morphology and the presence of elements of the synthesized nanoparticles were studied using by the scanning electron microscope (SEM) (JEOL JSM-6390LA, Japan) equipped with the EDX detector (Oxford X-MaxN, United Kingdom) at an appropriate accelerating voltage. The morphology, particle size and distribution of the AgNPs were further examined by a JEOL JEM-2100, Japan high resolution transmission electron microscope (HRTEM) at 200 kV. Powder diffraction was employed to investigate the crystallographic properties of the nanoparticles. Particle size was determined directly from the TEM images.

MTT assay and IC_{50} determination

The cytotoxic properties of the biosynthesized AgNPs of *Wrightia tinctoria* pod was studiedby performing MTT assay on 3T3-L1 cells. Briefly, cells were seeded in the 96-well microtitre plates with culture medium (250 mL) at the density of 2×10^4 cells/well and then cultured at at 37°C overnight for 24 h to reach about 60–70% confluency. Fresh medium with different AgNPs concentration was then used for the cell growth, and the control cells were grown in fresh culture medium. At least three wells of each treatment/control were retained and exposed for the established time period. After treatment, 100 µl of MTT solution (5 mg/mL, PBS) and fresh medium (100 mL) were poured into each well. The plates were then incubated 37°C for 4 h in the incubator where formazan crystals were formed by metabolically active cells. Next, the medium was removed carefully and 200 µL of the solvent dimethyl sulfoxide (DMSO) was placed in each well to dissolve the formazan crystals. The absorbance was measured within 30 min after the addition of the DMSO after the incubation at room temperature for 10 min by using a microplate reader at 540-570 nm. Viability of cells was represented as comparative percentage of the control (untreated) and the IC_{50} value was finalized from the concentration–response curve by calculations.

Differentiation of 3T3-L1 cells to adipocytes and Oil red O staining

The protocol describes the process of chemically inducing preadipocytes (3T3-L1) to differentiate into adipocyte-like cells using IBMX, (3-isobutyl-1-methylxanthine), dexamethasone and insulin. The method is widely used in metabolic and obesity research to model adipogenesis in vitro, and is adapted from [23]. Differentiated 3T3-L1 cells were used to assess the anti-adipogenic effect of the *Wrightia tinctoria* pod-mediated silver nanoparticles (AgNPs). Stock solutions of 3-isobutyl-1-methylxanthine (IBMX, 10 mM in DMSO) and dexamethasone (20 µM in distilled water) were made and insulin was prepared freshly. The differentiation induction medium (MDI medium) consisted of DMEM containing IBMX, dexamethasone and insulin at final concentrations of 0.5 mM, 1 µM and 10 µg/mL, respectively. The 3T3-L1 cells were transferred in a six-well plate at 3×10^3 cells/cm^2 and grown in DMEM for approximately 70% confluency by, changing the medium every 2–3 days until then. The growth media was replaced by 1 mL of MDI induction media per well (Day 0) to start adipogenic differentiation. Appropriate untreated cells were kept as controls and various concentrations of the synthesized AgNPs were simultaneously treated on the cells. On day 3 MDI medium was changed to insulin medium. The cells which underwent differentiation were microscopically analysed on day 5 to observe the morphologic changes and formation of droplets of lipids. The culture was then continued and on day 7, fresh culture medium (500µL/well) was added. For the Day 8 experiment, the degree of lipid accumulation was determined by staining both the treated and untreated differentiated cells by the staining procedure of Oil Red O and then visualizing under the microscope. After staining, the stained cells were fixed by employing the isopropanol followed by quantitative analysis of lipid accumulation in a 96-well plate.

Results and Discussion

Production of Silver Nanoparticles (AgNPs) Using *Wrightia tinctoria* pod extracts and UV–Visible Spectroscopic Confirmation

A visible change of the colour of the solution was initially observed as a preliminary indicator for AgNPs synthesis using the pod extract of *Wrightia tinctoria*. When silver nitrate solution was added to the plant extract the reaction mixture turned initially light brown which further turned to dark brown with silver grey appearance (Fig. 1).

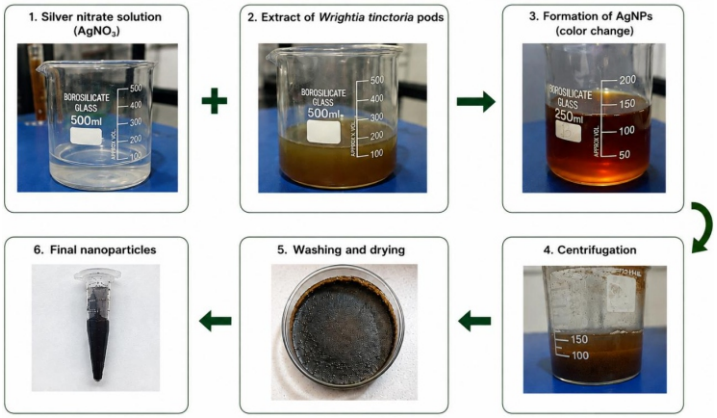

Figure 1: The experimental procedure involved in the green synthesis of Wrightia tinctoria mediated silver nanoparticles (AgNPs).

This visible colour change indicated preliminary evidence of the reduction of silver ions (Ag^+) to silver (Ag^0) and the subsequent formation of AgNPs. Nanoparticles can be synthesized using plant-mediated methods where the phytochemicals present in the plant extract can serve as reducing as well as stabilizing agents. Phenolics, flavonoids, terpenoids, and other reducing biomolecules may donate electrons to the silver ions, which may cause the change of silver ions into nanosized metallic silver [24]. Phytochemical screening of the methanolic extract of the pods of *Wrightia tinctoria* indicated the presence of alkaloids terpenoids, phenols and saponins. The positive Dragendorff's test suggested the presence of alkaloid constituents, but these were not identified individually by the present qualitative screening. Meanwhile, biomolecules found on the surface of the nanoparticles can also help to stabilize them and inhibit over-aggregation. The formation of AgNPs was further investigated by UV–visible spectroscopy in the range of 400–800 nm. The UV–visible spectrum of the reaction mixture revealed a sharp peak at around 425 nm [7]. This absorption band is a well-known characteristic of the surface plasmon resonance (SPR) attributed to AgNPs and therefore the appearance of this band is a spectroscopic confirmation of AgNPs formation. But the UV–visible spectroscopy alone does not give the complete information about the size, morphology, crystallinity, surface chemistry, and colloidal stability of the synthesized nanoparticles. Thus, the colour change and typical SPR band at 425 nm strongly suggest the formation of AgNPs, which requires more characterization studies to comprehensively determine the physicochemical properties of the AgNPs. The synthesized *W. tinctoria* pod-mediated AgNPs were then subjected to further characterization by suitable analytical techniques to determine functional groups, crystalline nature, morphology, particle size and surface characteristics of the synthesized AgNPs.

FTIR Characterization of *Wrightia tinctoria* Pod-Mediated AgNPs

FTIR analysis was conducted to identify the functional groups that are involved in the biosynthesized AgNPs and to understand the possible involvement of phytochemicals present in the *Wrightia tinctoria* pod extract that could be responsible for the reduction and stabilization process of AgNPs. As demonstrated from the FTIR spectrum, the nanoparticles exhibited a number of absorption bands, which correspond to the presence of various biomolecular functional groups attached to or associated with the synthesized nanoparticles. A wide absorption band was seen between about 3200 and 3600 cm^{-1}, possibly related to the stretching of the O–H bond [24]. These wide bands are typical for plants containing hydroxyl groups such as phenolics, alkaloids, alcohols and other plant metabolism products. In particular, the presence of biomolecules containing hydroxyl groups is especially relevant in the synthesis of green nanoparticles as the biomolecules can be involved in the reduction of Ag^+ ions to metallic Ag^0. Furthermore, biomolecules with hydroxyl groups could still be chemically bound to the surface of the nanoparticles and help to stabilize the nanoparticles. The band at 2913.99 cm^{-1} is related to stretching vibration mode of aliphatic C–H bonds especially C–CH_2 and C–CH_3 bonds [25]. These functional groups can be from different organic components of the pod extract of *W. tinctoria*. The occurrence of them in the spectrum indicates that biomolecules obtained from plants are related to the synthesized nanoparticles. There was a strong band around 1568.45 cm^{-1}.

Depending on the composition of the sample, this region can be linked to vibrations of the C = C groups, carbonyl-containing compounds, N–H bending vibrations [26]. During the process of forming nanoparticles in plant extract, biomolecules can interact with silver ions and the resulting mixture of phenolic compounds, alkaloids, proteins, and other secondary metabolites might be different for each extraction. Thus, the bands in this region could be attributed to the presence of these compounds in the reduction process and/or to capping of the nanoparticles' surface. The absorption band at 1349.32 cm-1 could be assigned to C–N or C–O stretching vibrations for organic molecules derived from the plants [27]. This finding also adds to the biomolecules found on the surface of the AgNPs from the pod extract. These compounds have surface activity and may act as natural stabilizers and prevent the nanoparticles from excessive aggregation. The band at 981.62 cm-1 is located in the fingerprint region of the FTIR spectrum and could correspond to the vibrations of C–O, C–H deformation, or any other type of vibration in organic compounds [28]. This band also shows that the phytochemical components in the pod extract of *W. tinctoria* are not separated from the NP preparation. In general, the overall FTIR spectrum indicates the presence of different functional groups of biomolecules of plants (Fig. 2).

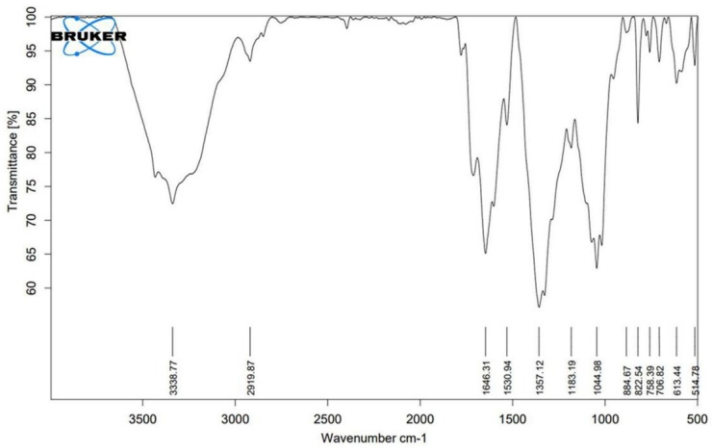

Figure 2: FTIR analysis of the functional groups which show the reduction and stabilization of nanoparticles in Wrightia tinctoria mediated silver nanoparticles

The results corroborate the role of phytochemicals present in the pods of *Wrightia tinctoria* in the green synthesis of AgNPs. The biomolecules such as phenolics and other reducing biomolecules could help to convert silver ions to metallic silver while organic molecules that remain on the surface of the nanoparticle could act as capping agents and stabilizers.

XRD analysis of green synthesised AgNPs

The crystal structure of the AgNPs prepared using the extract of *Wrightia tinctoria* pods was studied by X-ray diffraction (XRD). The diffractogram showed several distinct and sharp diffraction peaks, demonstrating the crystalline nature of the synthesized nanoparticles. The major diffraction peaks were observed at 2θ values of 28.378°, 38.154°, 40.558°, 44.339°, 64.486°, and 77.437°. Of these, the strongest diffraction peak was measured at 38.154° having a relative intensity of 100%, which suggests that this was the main crystalline reflection present in the sample [29]. Additional prominent peaks were observed at 44.339°, 64.486°, and 77.437°, with relative intensities of 35.3%, 17.7%, and 13.4%, respectively. The Cu radiation with a wavelength of 1.54060 Å was used for the XRD scan in the 2θ range of 10–80°.

The characteristic reflections seen at around 38.15°, 44.34°, 64.49° and 77.44° are characteristic reflections that are ordinarily observed for a crystalline metallic silver, and are characteristic reflections of face-centred cubic (FCC) silver. The 38.154° reflection intensity is very high, which is a sign of high crystallinity of the synthesized AgNPs. The presence of sharp and well-defined peaks further implies that the green synthesis mediated by the extract of *W. tinctoria* pods did not produce an amorphous silver containing material, instead, crystalline silver nanostructures were formed. The d-spacing values corresponding to the major peaks were 2.35681 Å at 38.154°, 2.04135 Å at 44.339°, 1.44383 Å at 64.486°, and 1.23151 Å at 77.437°. The values also help to confirm the crystalline nature of the synthesized material. A small peak was also detected at 28.378 and a weak peak at 40.558. Small additional peaks might be due to residual phytochemicals from the plant extract, minor crystalline species or other phase associated with the sample. These minor peaks must therefore be taken with a grain of salt and can be identified as metallic silver only, if at all, when compared with an appropriate standard diffraction data base. The crystallite sizes calculated using the peak broadening of XRD was found to be about 99.9 nm, 84.5 nm and 94.2 nm at the reflections at approximately 38.155°, 44.339° and 64.483°, respectively, indicating an average crystallite size of about 93 nm (Fig. 3).

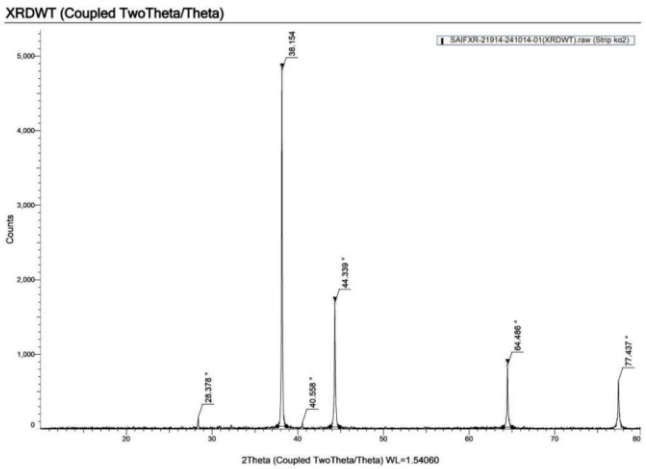

Figure 3: X-ray Diffraction (XRD) pattern of biosynthesized silvernanoparticles prepared by using Wrightia tinctoria pod extract

The results show that the synthesized material had been nanocrystalline. The crystallite size measured by XRD is to be noted as the size of coherently diffracting crystalline domains and could be different from the particle size measured by SEM, TEM or dynamic light scattering analysis. Thus, XRD results indicate that the extract from the *Wrightia tinctoria* pods used in this synthesis method yielded mainly crystalline AgNPs. The sharp reflections and the dominant peak at 38.154° are good indicators of the crystallinity of the AgNPs synthesized. The pod extract might have acted in two ways, allowing reduction of the silver ions, and also, stabilizing the crystalline nanoparticles [30].

3.4 EDX Analysis of *Wrightia tinctoria*-Mediated AgNPs

The elemental composition of the AgNPs prepared by the extraction of the pods of *Wrightia tinctoria* was investigated by energy-dispersive X-ray spectroscopy (EDX).

The EDX spectra from various selected sites revealed a strong and consistent peak in the region of 3 keV, which corresponds to silver (Ag) indicating that silver is the major elemental component of the synthesized nanoparticles [31]. In all analysed spectra, a strong Ag peak is observed, which further confirms the successful reduction of the Ag ions and formation of AgNPs. A few small peaks were also seen corresponding to oxygen (O) and carbon (C) (Fig 4).

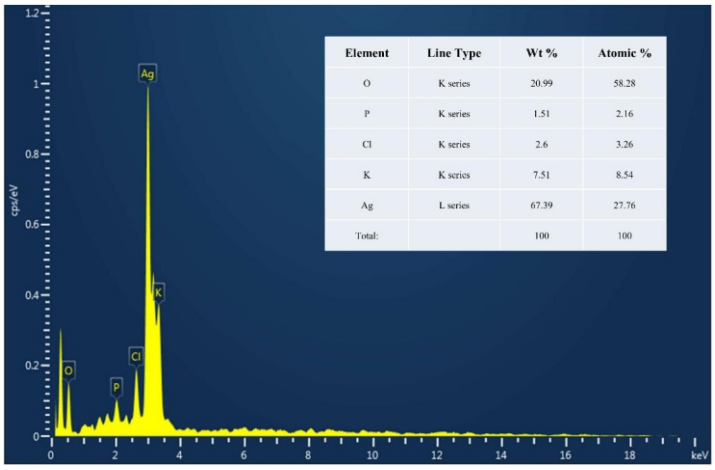

Figure 4: The energy-dispersive X-ray (EDX) spectrum of biosynthesized silver nanoparticle prepared using the extract of the pods of Wrightia tinctoria.

The presence of these elements could be linked to phytochemicals found in *W. tinctoria* pod extract which were adsorbed on the surface of the nanoparticles which indicates their potential role as reducing and capping agents [32]. Some of these detections of weak signals for potassium (K) and phosphorus (P) can be from naturally occurring mineral in the plant extract or residual from sample preparation [33]. The abundance of the Ag signal at all of the sites analyzed suggests that the synthesized material contained a high concentration of silver. In conclusion, the EDX results along with UV-visible, FTIR and XRD analyses, is an additional proof of the green synthesis of AgNPs using *Wrightia tinctoria* pods.

Scanning electron microscopy of synthesized AgNPs

The surface morphology and particle properties of the AgNPs synthesized using the extract of the *Wrightia tinctoria* pod was investigated by scanning electron microscopy (SEM) at different magnifications (×500, ×10,000). The SEM images showed that a heterogeneous particulate material comprised of irregular particles with rough and irregular surface morphology was formed. Synthesized material at lower magnifications (×500 to ×1,500) was seen as dense clusters and aggregated masses that were distributed throughout the observed field. The synthesized AgNPs tended to cluster together into a number of the smaller particulate structures forming these aggregates. The morphology of synthesized particles became more obvious at the intermediate magnifications of ×3,500 and ×7,000. The particle shapes were mostly irregular, granular and quasi-spherical, but a completely uniform particle shape could not be identified in the entire sample. The particles were very compact and clustered in various sizes. This is a common phenomenon in the synthesis of nanoparticles using plants. Variations in reducing and capping biomolecules can affect the process of nucleation, growth, and aggregation of nanoparticles in the plant [34]. The phytochemicals in the *W. tinctoria* pod extract thus could have participated in both the reduction of silver ions, as well as the stabilization of the resultant nanoparticles [35].

A SEM image was obtained at ×10,000 magnification which gave a better image of the particle aggregates. From the measurements indicated on the micrograph, the dimensions measured ranged from about 240.83 to 541.48 nm, with intermediate dimensions of 325.58 nm and 428.02 nm (Fig. 5).

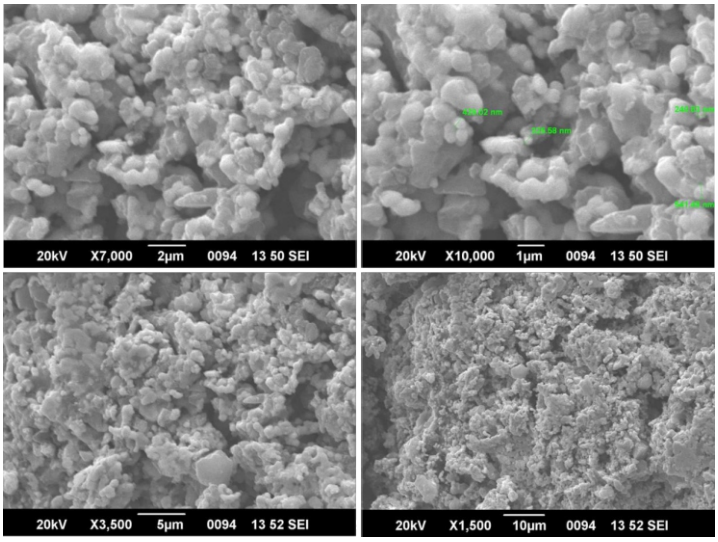

Figure 5: High resolution scanning electron microscopy (SEM) images of Wrightia tinctoria mediated silver nanoparticles at various magnifications revealed particle aggregation and heterogeneous morphology of the particles. Scale bars are shown in each micrograph

The values show that the structures observed by SEM were mainly submicron sized aggregates, not individual nanoparticles, the mean dimensions of the four marked structures were ~384 nm. The strong aggregation in the SEM images could be due to the synthesis, centrifugation, drying or preparation process [36]. Interparticle interactions can bring the nanoparticles close to one another during drying, and result in larger aggregates [37]. Moreover, biomolecules from *W. tinctoria* pod extracts and associated with the surface of a nanoparticle can also play a role in the creation of more complex agglomerated structures. Thus, the particle sizes obtained from SEM cannot automatically be taken as the size of the individual primary nanoparticles.

Transmission electron microscopy of green synthesized AgNPs

Transmission electron microscopy (TEM) was also used to investigate the morphology, size and distribution of the AgNPs synthesized by the extract of *Wrightia tinctoria* pods. The TEM micrographs showed clearly the formation of nanosized particles with a morphology mostly spherical to quasi-spherical. Most of the particles appeared almost spherical, but there were also some irregularly shaped particles observed reflecting some morphological heterogeneity. The nanoparticles looked like dark electron-dense particles scattered across a relatively light background at different magnifications. The darker contrast is consistent with the presence of electron-dense silver-containing nanoparticles. The particles were found in both as individual and small clusters that meant moderate aggregation. The presence of much smaller primary nanoparticles was observed using TEM, but not larger agglomerated structures observed in SEM [38]. The particle size analysis was carried out on the TEM micrographs and the synthesized nanoparticles were found to be in the range of around 19.97-43.89 nm.

The measured particles included sizes of approximately 19.97, 20.69, 21.43, 23.52, 27.78, 29.92, 32.54, 32.93, 33.14, 34.87, 35.36, 39.26, and 43.89 nm. From these measurements, the average particle size measured is about 30.4 nm. The results thus, validate the synthesis of nanoparticles in the nanoscale range using the extract of the pod of *W. tinctoria*. The relatively large structures (from about 240 nm to 541 nm) observed by SEM were found to be considerably smaller than the primary nanoparticles (mainly 20 to 44 nm) revealed by TEM (Fig 6).

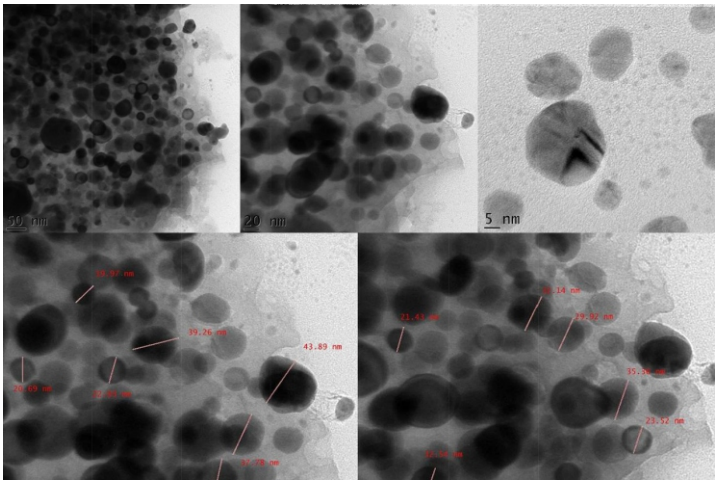

Figure 6: The silver nanoparticles were synthesized using Wrightia tinctoria pod and characterized by transmission electron microscopy (TEM) micrographs. Scale bars are given in each micrograph

This difference indicates that the bigger size structures seen under SEM do not seem to be single particles, but rather aggregates or agglomerates of several smaller nano-size particles. This can be due to aggregation during centrifugation, during drying, or during sample preparation [39]. The average crystallite size, obtained from the XRD was also higher than the nanoscale dimensions observed by TEM, which indicates that the two characterization techniques measure different structural features and hence may not yield the same size values. TEM allows for the direct identification of individual particles, while XRD can be used to estimate the size of coherent crystalline domains and SEM can primarily give information on the morphology of particle aggregates [40].

Cytotoxicity Assessment of *Wrightia tinctoria*-Mediated AgNPs by MTT Assay

The 3T3-L1 cell line was used for a MTT assay to determine the cytotoxic effect of the green synthesized AgNPs at different concentrations [41]. The assay showed to be concentration-dependent and resulted in a decrease in cell viability, especially at high concentrations of synthesized nanoparticles. The calculated IC_{50} value was 119.7µg/mL while the calculated dose-response analysis showed that approximately 50% inhibition of cellular viability was achieved around this concentration (Fig 7).

The cells maintained relatively high viability at lower concentration of the nanoparticles (10 – 40 µg/mL), which indicates comparatively lower cytotoxic effects at these concentrations. The viability of the cells decreased as the concentration of the nanoparticles increased, with a significant decrease in cell viability above about 40-60 µg/mL. The cell viability at the treatment concentrations of 60, 120, and 180 µg/mL was still significantly lower than that at the lower doses implying the strong effect of exposure of nanoparticles on the metabolic activities of cells [42].

The MTT results were also confirmed by microscopic examination of treated 3T3-L1 cells (Fig 8). The cells showed mostly normal morphology and distribution at low concentrations of AgNPs. But as the concentration of the nanoparticles increased, changes in the cell density and morphology were also clearly observed. Cell density decreased, and cellular stress and/or damage were seen at higher concentrations (240, 300 and 400 µg/mL) (Fig 8).

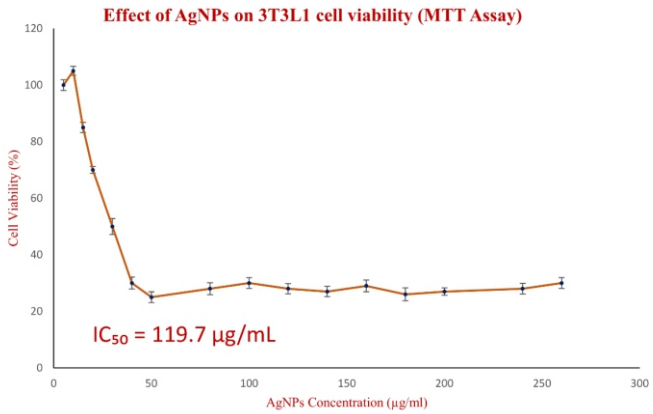

Figure 7: Calculation of IC_{50} value using MTT assay. Experimental values were based on three times repetition and are represented as mean ± S.D

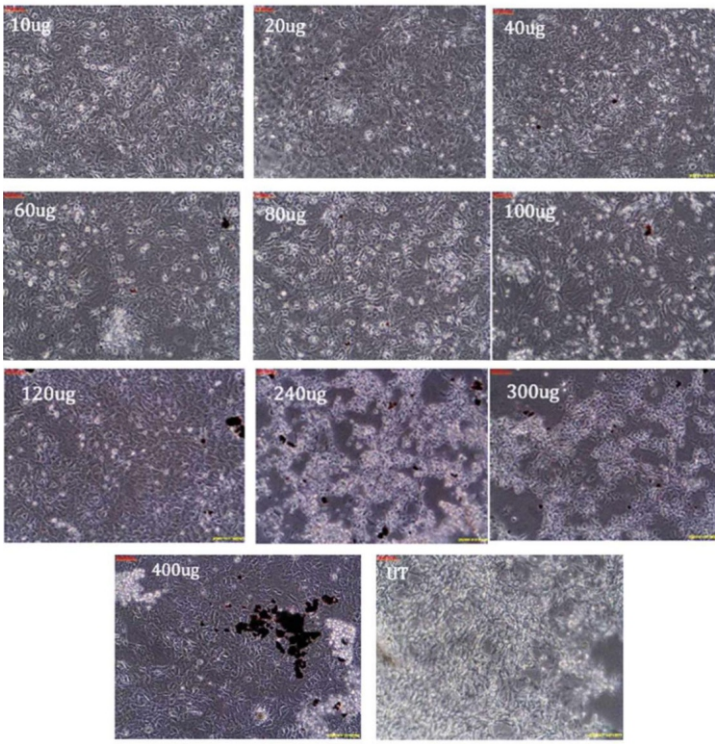

Figure 8: Dose-dependent effect of Wrightia tinctoria pod-mediated silver nanoparticles on the viability of 3T3-L1 cells

The morphological changes were in line with the decrease in metabolic activity observed using the MTT assay [43]. The reduction of MTT is a reflection of the reduction of the metabolic activity of live cells after being exposed to the synthesized nanoparticles. The cytotoxic response can be correlated with the interactions between AgNPs and the cellular environment, such as possible oxidative stress and change in mitochondrial activity [44]. The synthesized particles are in the nano-scale, as determined by TEM analysis (most of the particles are in the range of about 20–44 nm), which can enhance their interaction with cells and affect their biological activity [45]. Interestingly, the viability values at intermediate and higher concentrations were not completely linear according to dose.

This variability can be due to variations in the aggregation/sedimentation of nanoparticles, cellular adaptation, or experimental variation [46]. Thus, it is recommended to use a non-linear dose-response regression model, not a linear trendline, to determine the IC_{50}. Overall, the MTT assay showed that the AgNPs loaded in *Wrightia tinctoria* pods have concentration-dependent cytostatic effects on 3T3-L1 cells, with an IC_{50} of 119.7 µg/mL. Considering the results, concentrations lower than the IC_{50} can be used for further experiments to study the biological effects of the nanoparticles, such as their effects on adipocyte differentiation and lipid accumulation.

Anti-adipogenic Activity of *Wrightia tinctoria*-Mediated AgNPs Assessed by Oil Red O Staining

Anti-adipogenic activity of *Wrightia tinctoria* pod mediated AgNPs was assessed in differentiated 3T3-L1 adipocytes with Oil Red O staining. Oil Red O is a lipid-soluble dye that can be used to stain intracellular neutral lipids and lipid droplets to help visualize the level of lipid accumulation in adipocytes [47]. Intracellular lipid accumulation was evident in the untreated control cells, which were indicative of successful adipogenic differentiation and lipid droplet formation. However, there was visible decrease in lipid accumulation in the AgNPs treated group at 80, 100 and 120 µg/mL. The synthesized nanoparticles were shown to have a significant effect on the reduction of lipid accumulation through spectrophotometric quantification of Oil Red O staining. Relative lipid accumulation was 57.17%, 45.18% and 42.00% in the 80, 100 and 120 µg treatments, respectively, compared with the untreated treatment (normalized to 100%).

The lowest level of lipid accumulation was at a dose of 120 µg, which resulted in the maximum reduction in intracellular lipid deposition. The results overall confirm the anti-lipogenic effect of the synthesized nanoparticles in a dose-dependent manner, with the highest inhibitory effect observed at a dose of 120 µg (Table 1).

Table 1: Relative intracellular accumulation of lipid in 3T3-L1 cells following the treatment with biosynthesized silver nanoparticles as assessed by Oil Red O staining. All values are reported as mean values ± S.D

Sr. No.	Treatment	Relative Lipid Accumulation (%)
1	Control	100
2	80	57.17 ± 2.4
3	100	45.18 ± 0.4
4	120	42 ± 0.3

As the concentration of the nanoparticles increased, the extent of reduction in Oil Red O staining increased, indicating that the effect of nanoparticles on the inhibition of the deposition of lipids into the cells was concentration dependent. Similar trend was observed with the gold nanoparticles on adipogenic differentiation of human mesenchymal stem cell [48]. These were supported by microscopic examination. Lipid droplet accumulation and changes in the normal lipid-rich characteristic morphology of differentiated adipocytes were observed to be decreased in AgNPs-treated cells when compared to the control. It was more pronounced at 100 and 120 µg/mL, in which the intensity and distribution of intracellular lipid staining seemed to be smaller than in the untreated control (Fig 9).

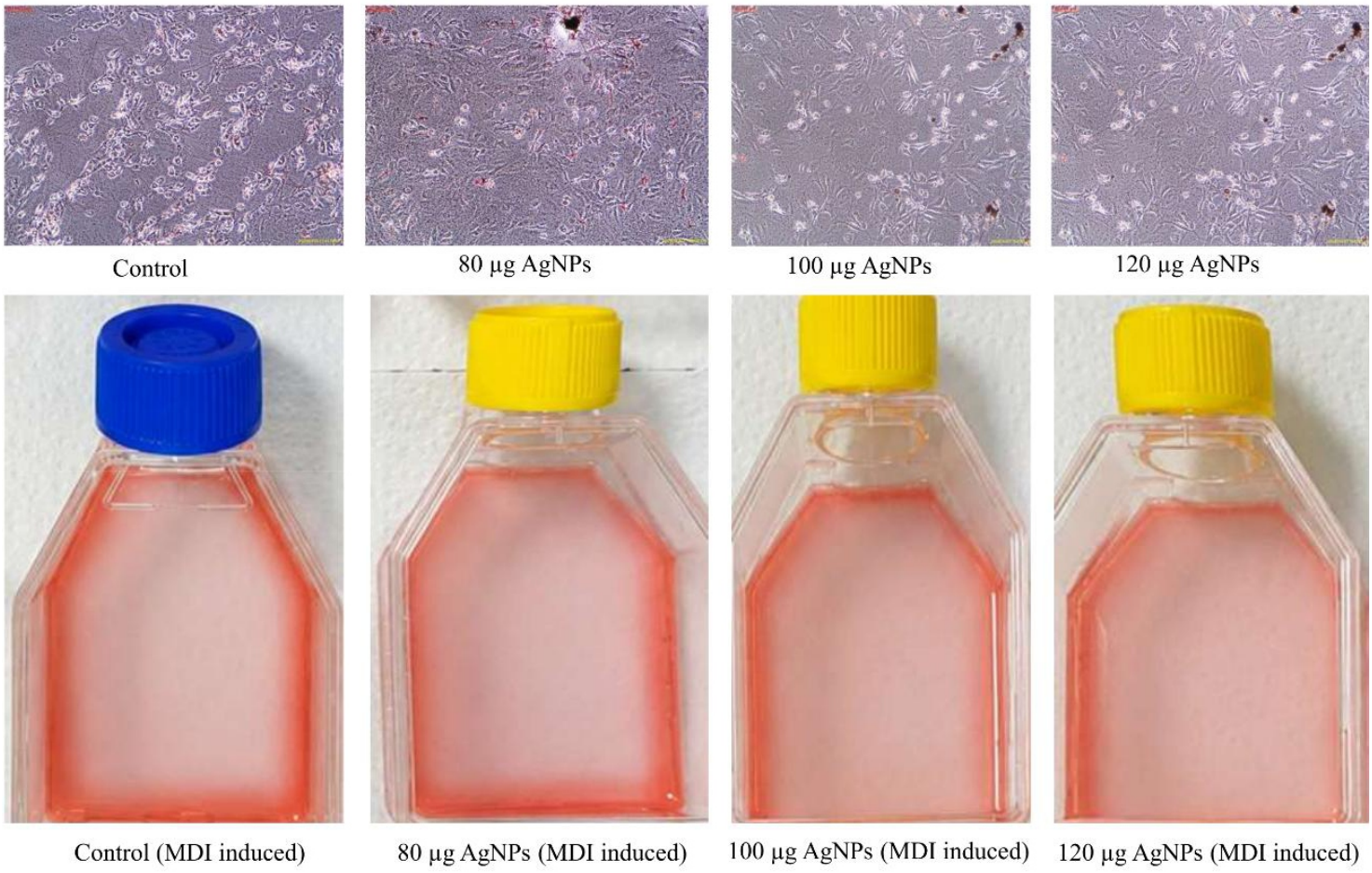

Figure 9. Differentiated 3T3-L1 adipocytes treated with different concentrations of oil red O-stained Wrightia tinctoria pod mediated silver nanoparticles and its intracellular lipid accumulation compared with untreated differentiated control. MDI stands for Differentiation induction medium.

The decreased lipid accumulation could suggest that the *W. tinctoria*-mediated AgNPs affect the differentiation of adipocytes and/or lipid storage in the cells. The synthesized AgNPs and the bioactive phytochemicals attached to the surface of AgNPs may be linked with this anti-adipogenic effect [49]. This anti-adipogenic effect may be attributed to the nanosized properties of the prepared AgNPs and the attached bioactive phytochemicals [49].

Conclusion

Green synthesis of silver nanoparticles (AgNPs) was achieved using an extract of *Wrightia tinctoria* pods, and preliminary biological activity studies were conducted in 3T3-L1 cells. The visible colour change from light brown to dark brown colour and characteristic UV-vis absorption peak at ~425nm highlighted the formation of AgNPs. FTIR analysis also indicated possible involvement of functional groups from the plants in the preparation of silver nanoparticles: The prescription method of the preparation of silver nanoparticles involved the use of plant phytochemicals, which were suggested by FTIR analysis. The synthesized material was confirmed to be crystalline by XRD analysis, showing characteristic reflections of crystalline metallic silver with an average crystallite size of ~93nm. Strong silver signal was observed around 3 keV, revealed by EDX analysis, indicating that silver is the primary elemental component. SEM showed that the particulate structures were heterogeneous and aggregated while TEM showed the presence of a quasi-spherical to spherical primary particulate structures with an average size of 30.4 nm (with a range of 19.97 to 43.89 nm). The difference between SEM and TEM measurements suggests that the larger structure seen in SEM may have been aggregates of smaller nanoparticles. The synthesized AgNPs were found to have an inhibitory effect on 3T3-L1 cell viability in a concentration-dependent manner, through the biological evaluation with estimated IC_{50} value of 119.7 µg/mL. Importantly, concentrations below the IC_{50} resulted in a visible decrease in intracellular lipid accumulation in differentiated 3T3-L1 adipocytes as assessed by Oil Red O staining. This reduction was more striking at 100 and 120 µg/mL, which could indicate possible inhibitory effects on adipocyte differentiation and/or lipid storage. In general, the pods extract of *W. tinctoria* is a potential plant-based reducing and stabilizing agent for the synthesis of AgNPs with a biological activity. The synthesized nanoparticles had appropriate physicochemical properties, and had some preliminary anti-adipogenic activity in 3T3-L1 cell model. To prove the mechanism of the anti-adipogenic properties observed, however, further quantitative analysis of lipid accumulation and molecular studies on adipogenic regulators such as PPARγ, adiponectin, C/EBPα, SREBP-1c and FAS should be performed [50].

Acknowledgement

Arpana Ashokrao Durge would like to thank Dr. Ambedkar College, Deekshabhoomi for allowing the use of research and tissue culture facilities. The author would also like to thank Miss Pooja Kadu for her help in procuring 3T3-L1 cell lines.

References

1. Piché ME, Tchernof A, Després JP. Obesity phenotypes, diabetes, and cardiovascular diseases. *Circ Res*. 2020;126(11):1477-1500.
2. Longo M, Zatterale F, Naderi J, Parrillo L, Formisano P, Raciti GA, et al. Adipose tissue dysfunction as determinant of obesity-associated metabolic complications. *Int J Mol Sci*. 2019;20(9):2358.
3. Moseti D, Regassa A, Kim WK. Molecular regulation of adipogenesis and potential anti-adipogenic bioactive molecules. *Int J Mol Sci*. 2016;17(1):124.
4. Guru A, Issac PK, Velayutham M, Saraswathi NT, Arshad A, Arockiaraj J. Molecular mechanism of down-regulating adipogenic transcription factors in 3T3-L1 adipocyte cells by bioactive anti-adipogenic compounds. *Mol Biol Rep*. 2021;48(1):743-761.
5. Soong TC, Lee KT, Hsu YC, Tsai TH. Cucurbitacin E suppresses adipogenesis and lipid accumulation in 3T3-L1 adipocytes without cytotoxicity. *Biomedicines*. 2025;13(8):1826.
6. Zhang XF, Liu ZG, Shen W, Gurunathan S. Silver nanoparticles: synthesis, characterization, properties, applications, and therapeutic approaches. *Int J Mol Sci*. 2016;17(9):1534.
7. Durge AA, Dongre U, Moon UR. Antimicrobial activity of silver nanoparticles synthesized from *Wrightia tinctoria* fruit extracts. *Environ Conserv J*. 2024;25(1):16-21.
8. Abhimanyu P, Arvind M, Kishor N. Biosynthesis of CuO nanoparticles using plant extract as a precursor: characterization, antibacterial, and antioxidant activity. *Nano Biomed Eng*. 2023;15(4):369.
9. Sheikh S, Mungole AJ, Pandhurnekar CP, Kanfade HP, Pandhurnekar HC, Pawar AP. Greener synthesis of copper oxide nanoparticles using *Rivina humilis* L. plant extract, characterization and their biological evaluation for anti-microbial and anti-oxidant activity. *ChemistrySelect*. 2024;9(31):e202401219.
10. Pawar A, Mungole A, Naktode K. Biogenic copper oxide nanoparticles synthesized from whole plant extract of *Nicotiana plumbaginifolia* Viv.: characterization, antibacterial, and antioxidant properties. *J Turk Chem Soc A Chem*. 2024;11(3):1005-1016.
11. Skóra B, Piechowiak T, Szychowski KA. Dual mechanism of silver nanoparticle-mediated upregulation of adipogenesis in mouse fibroblasts (3T3-L1) in vitro. *Toxicol Appl Pharmacol*. 2023;479:116726.
12. Sheikh S, Mungole AJ, Bhat AR, Pawar AP, Pandhurnekar CP, Pandhurnekar HC, et al. Sustainable plant mediated synthesis of cobalt oxide nanoparticles using *Uraria picta* extract with enhanced biological activity. *Sci Rep*. 2025;15(1):44017.
13. Villagrán Z, Anaya-Esparza LM, Velázquez-Carriles CA, Silva-Jara JM, Ruvalcaba-Gómez JM, Aurora-Vigo EF, et al. Plant-based extracts as reducing, capping, and stabilizing agents for the green synthesis of inorganic nanoparticles. *Resources*. 2024;13(6):70.
14. Yadav S, Nadar T, Lakkakula J, Wagh NS. Biogenic synthesis of nanomaterials: bioactive compounds as reducing, and capping agents. In: *Biogenic Nanomaterials for Environmental Sustainability: Principles, Practices, and Opportunities*. Cham: Springer International Publishing; 2024. p. 147-188.
15. Kafesa A, Baehaki F. Green synthesis of silver nanoparticles. In: *Silver Nanoparticles-Fundamentals, Properties, Synthesis, and Applications*. IntechOpen; 2026. doi:10.5772/intechopen.1014807.
16. Simon S, Sibuyi NR, Fadaka AO, Meyer S, Josephs J, Onani MO, et al. Biomedical applications of plant extract-synthesized silver nanoparticles. *Biomedicines*. 2022;10(11):2792.
17. Shankar SR, Rangarajan R, Sarada DVL, Kumar CS. Evaluation of antibacterial activity and phytochemical screening of *Wrightia tinctoria* L. *Pharmacogn J*. 2010;2(14):19-22.
18. Rizzatti V, Boschi F, Pedrotti M, Zoico E, Sbarbati A, Zamboni M. Lipid droplets characterization in adipocyte differentiated 3T3-L1 cells: size and optical density distribution. *Eur J Histochem*. 2013;57(3):e24.
19. Ko JH, Nam D, Um JY, Jung SH, Ahn KS. Bergamottin inhibits adipogenesis in 3T3-L1 cells and weight regulation in diet-induced obese mice. *Am J Chin Med*. 2018;46(3):601-615.
20. Revi N, Oladejo OD, Bijukumar D. In vitro, in vivo and ex vivo models for toxicity evaluation of nanoparticles: advantages and disadvantages. In: *Toxicity of Nanoparticles-Recent Advances and New Perspectives*. IntechOpen; 2023.

21. Patil US, Adireddy S, Jaiswal A, Mandava S, Lee BR, Chrisey DB. In vitro/in vivo toxicity evaluation and quantification of iron oxide nanoparticles. *Int J Mol Sci*. 2015;16(10):24417-24450.
22. Krug HF, Wick P. Nanotoxicology: an interdisciplinary challenge. *Angew Chem Int Ed Engl*. 2011;50(6):1260-1278.
23. Reed BC, Lane MD. Expression of insulin receptors during preadipocyte differentiation. *Adv Enzyme Regul*. 1980;18:97-117.
24. Ossowski S, Rybak K, Pobiega K, Sękul J, Domżalska Z, Gregorek K, et al. Antioxidant activity and microbial quality of freeze-dried, lactic acid fermented peach products. *Molecules*. 2025;30(11):2360.
25. Yue WA, Xing FA. Functional groups of sequential extracts and corresponding residues from Hefeng sub-bituminous coal based on FT-IR analysis. *J Fuel Chem Technol*. 2021;49(7):890-901.
26. Obode OC, Olayemi SO, Odu IG, Alake OT, Akinola OS, Obiechefu AU. Comparative study of extracts from *Phoenix dactylifera* using Fourier Transform Infrared (FTIR) spectroscopy: unveiling phytochemical diversity. *SSR J Med Sci*. 2025;2(7):39-45.
27. Yusuf MO. Bond characterization in cementitious material binders using Fourier-transform infrared spectroscopy. *Appl Sci*. 2023;13(5):3353.
28. Azeez S, Shenbagaraman R. Fourier transform infrared spectroscopy in characterization of bionanocomposites. In: *Characterization Techniques in Bionanocomposites*. Woodhead Publishing; 2025. p. 209-227.
29. Alshareef M, Alharbi A, Ahmed S, Mahmoud AM, Fahmi MS, Ali ME, et al. Synthesis of silver sulfide acanthite phase nanoparticles for photothermal hybrid PSF membrane. *Chem Eng Res Des*. 2025;214:415-426.
30. Raja S, Ramesh V, Thivaharan V. Antibacterial and anticoagulant activity of silver nanoparticles synthesised from a novel source-pods of *Peltophorum pterocarpum*. *J Ind Eng Chem*. 2015;29:257-264.
31. Jyoti K, Baunthiyal M, Singh A. Characterization of silver nanoparticles synthesized using *Urtica dioica* Linn. leaves and their synergistic effects with antibiotics. *J Radiat Res Appl Sci*. 2016;9(3):217-227.
32. Bayat M, Zargar M, Astarkhanova T, Pakina E, Ladan S, Lyashko M, et al. Facile biogenic synthesis and characterization of seven metal-based nanoparticles conjugated with phytochemical bioactives using *Fragaria ananassa* leaf extract. *Molecules*. 2021;26(10):3025.
33. Chuparina EV, Revenko AG. Application of X-ray spectral analysis in Russia to determine chemical elements in medicinal plants. *J Anal Chem*. 2024;79(12):1679-1693.
34. Edo GI, Mafe AN, Ali AB, Akpoghelie PO, Yousif E, Isoje EF, et al. Green biosynthesis of nanoparticles using plant extracts: mechanisms, advances, challenges, and applications. *BioNanoSci*. 2025;15(2):267.
35. Amutha E, Sivakavinesan M, Rajaduraipandian S, Annadurai G. Identification of phytochemicals capping the biosynthesized silver nanoparticles by *Wrightia tinctoria* and evaluation of their in vitro antioxidant, antibacterial, antilarvicidal, and catalytic activities. *Emerg Mater*. 2023;6(2):525-534.
36. Ghomrasni NB, Chivas-Joly C, Devoille L, Hochepied JF, Feltin N. Challenges in sample preparation for measuring nanoparticles size by scanning electron microscopy from suspensions, powder form and complex media. *Powder Technol*. 2020;359:226-237.
37. Rahman IA, Vejayakumaran P, Sipaut CS, Ismail J, Chee CK. Effect of the drying techniques on the morphology of silica nanoparticles synthesized via sol-gel process. *Ceram Int*. 2008;34(8):2059-2066.
38. Larue C, Laurette J, Herlin-Boime N, Khodja H, Fayard B, Flank AM, et al. Accumulation, translocation and impact of TiO2 nanoparticles in wheat (*Triticum aestivum* spp.): influence of diameter and crystal phase. *Sci Total Environ*. 2012;431:197-208.
39. Hagendorfer H, Lorenz C, Kaegi R, Sinnet B, Gehrig R, Goetz NV, et al. Size-fractionated characterization and quantification of nanoparticle release rates from a consumer spray product containing engineered nanoparticles. *J Nanopart Res*. 2010;12(7):2481-2494.
40. Burleson DJ, Driessen MD, Penn RL. On the characterization of environmental nanoparticles. *J Environ Sci Health A*. 2004;39(10):2707-2753.
41. Kamalanathan J, Venkatesh R, Swetha S, Sampath S, Ahmed MZ, Alqahtani AS, et al. Microwave-assisted green synthesis of silver nanoparticles using *Cynoglossum furcatum* extract: biomedical evaluation against A431 skin cancer cell line. *Mater Technol*. 2024;39(1):2401260.
42. Liu N, Tang M. Toxic effects and involved molecular pathways of nanoparticles on cells and subcellular organelles. *J Appl Toxicol*. 2020;40(1):16-36.
43. Cruz EM, Concato VM, de Morais JM, Silva TF, Inoue FS, de Souza Cremer M, et al. Melatonin modulates the Warburg effect and alters the morphology of hepatocellular carcinoma cell line resulting in reduced viability and migratory potential. *Life Sci*. 2023;319:121530.
44. He J, Ma Y, Niu X, Pei J, Yan R, Xu F, et al. Silver nanoparticles induce endothelial cytotoxicity through ROS-mediated mitochondria-lysosome damage and autophagy perturbation: the protective role of N-acetylcysteine. *Toxicology*. 2024;502:153734.
45. Salem SS. A mini review on green nanotechnology and its development in biological effects. *Arch Microbiol*. 2023;205(4):128.
46. Cardoso BD, Souza A, Nobrega G, Afonso IS, Neves LB, Faria C, et al. Progress in nanofluid technology: from conventional to green nanofluids for biomedical, heat transfer, and machining applications. *Nanomaterials*. 2025;15(16):1242.
47. Daemen S, van Zandvoort MA, Parekh SH, Hesselink MK. Microscopy tools for the investigation of intracellular lipid storage and dynamics. *Mol Metab*. 2016;5(3):153-163.
48. Kohl Y, Gorjup E, Katsen-Globa A, Büchel C, von Briesen H, Thielecke H. Effect of gold nanoparticles on adipogenic differentiation of human mesenchymal stem cells. *J Nanopart Res*. 2011;13(12):6789-6803.
49. Prapaipittayakhun J, Arpornmaeklong P, Boonyuen S. Effects of biosynthesis *Oroxylum indicum*/silver nanoparticles on biological behaviors of the encapsulated stem cells [dissertation]. Thammasat University; 2022.
50. Hadrich F, Sayadi S. Apigetrin inhibits adipogenesis in 3T3-L1 cells by downregulating PPARγ and CEBP-α. *Lipids Health Dis*. 2018;17(1):95.